Aggregation Equilibria of *Escherichia coli* RNA Polymerase: Evidence for Anion-Linked Conformational Transitions in the Protomers of Core and Holoenzyme†

Sandra L. Shaner, David M. Piatt,‡ C. Glen Wensley,§ Hyuk Yu, Richard R. Burgess, and M. Thomas Record, Jr.*

ABSTRACT: The aggregation equilibria of *Escherichia coli* RNA polymerase core and holoenzyme have been studied by velocity sedimentation as a function of [NaCl] both in the presence and in the absence of $MgCl_2$. Effects of other anions (F^- and I^-), pH, and temperature have also been examined. Diffusion coefficients obtained by quasi-elastic light scattering (QLS) at high and low salt concentrations were used in conjunction with sedimentation coefficients under these conditions to obtain molecular weights of the protomer and aggregates of the core enzyme. At low salt concentration, core aggregates to a tetramer in the absence of $MgCl_2$ and to an octamer in the presence of $MgCl_2$. Some ambiguity exists in the interpretation of the sedimentation and QLS data for holoenzyme. The sedimentation results are consistent with the formation of dimers at low salt, both in the presence and in the absence of $MgCl_2$. In all cases, equilibrium constants were calculated assuming a simple monomer–*j*-mer stoichiometry. These equilibrium constants are extremely sensitive functions of the concentration and type of monovalent anion. In Cl^-, aggregation of both core and holoenzyme begins abruptly when the salt concentration is reduced below ~0.2 M (at a protein concentration of ~0.30 mg/mL); for core, substitution of I^- for Cl^- suppresses aggregation while F^- enhances aggregation at a fixed anion concentration. No specific effect of monovalent cations (Na^+, NH_4^+) is observed; Mg^{2+} has no effect on holoenzyme dimerization and has little effect on the salt range of core aggregation, though the stoichiometries of the core aggregates in the presence and absence of Mg^{2+} differ. Anion effects on these equilibria were modeled by assuming that a class of anion-binding sites on the protomer is not present in the aggregate, so that anion release accompanies aggregation. Analytical expressions for several models of the effect of anions on the aggregation equilibria were derived by using the method of binding polynomials. The salt dependence of the aggregation equilibria in the absence of Mg^{2+} appears inconsistent with a model in which the anion-binding sites on the protomer are independent (noncooperative), but it is well described by a model in which anion binding to the protomers occurs in a completely cooperative manner. The molecular basis of this apparent cooperative effect of anions on the aggregation equilibria is proposed to be an allosteric effect of anions on conformational equilibria of the protomers of core polymerase and the holoenzyme. Implications of such a salt-dependent conformational transition for the DNA-binding interactions of the enzyme are considered.

Escherichia coli RNA polymerase is a multisubunit enzyme occurring in two forms: holo (subunit structure $\alpha_2\beta\beta'\sigma$) and core[1] ($\alpha_2\beta\beta'$). Holoenzyme can be reversibly dissociated into core and the σ subunit (Burgess et al., 1969). The presence of σ is required for the specific and efficient initiation of RNA synthesis by RNA polymerase (Burgess, 1971; Chamberlin, 1976).

The ability of RNA polymerase to aggregate at low salt concentrations was noted quite early (Richardson, 1966; Stevens et al., 1966). This aggregation at low salt has been utilized as a key step in purifying RNA polymerase (Burgess, 1969). Berg & Chamberlin (1970) investigated the effect of ammonium sulfate concentration on the extent of aggregation of core, holoenzyme, and a 60% σ-saturated RNA polymerase in the presence of 0.01 M $MgCl_2$ using a velocity sedimentation assay. On the basis of the ratio of the $s_{20,w}$ obtained at the lowest ionic strength investigated to that obtained at high ionic strength, they concluded that at low ionic strength in the presence of Mg^{2+}, core polymerase forms aggregates at least as large as a hexamer while holoenzyme forms dimers.

Recently, there has been renewed interest in the aggregation of RNA polymerase as a result of the proposal that the extent of holoenzyme dimerization may be used in vivo as a mechanism to regulate the rate of transcription from various promoters (Travers et al., 1982). In addition, quantitative information on the aggregation equilibrium of core and holoenzyme is desirable as a practical guide to the extent of aggregation of the enzyme as a function of enzyme concentration and ionic conditions.

We have investigated the dependence upon solution conditions of the various aggregation equilibria in which the two forms of RNA polymerase participate. Preliminary studies (Wensley, 1977) indicated that Mg^{2+} had a profound effect on the stoichiometry of the aggregate and in addition suggested tha monovalent anions play a key role in dictating the extent of aggregation. We have quantified these ion effects, using sedimentation velocity to determine equilibrium constants as a function of solution conditions. (Others have indicated the difficulty of performing the more rigorous sedimentation equilibrium on this large, multisubunit protein; Berg & Chamberlin, 1970; R. R. Burgess, unpublished results.) Quasi-elastic light scattering (QLS) was used to determine diffusion coefficients of the protomer and low salt aggregates of core polymerase; molecular weights were obtained for these

† From the Department of Chemistry (S.L.S., D.M.P., C.G.W., H.Y., and M.T.R.), and the McArdle Laboratory for Cancer Research (R.R.B.), University of Wisconsin, Madison, Wisconsin 53706. *Received January 26, 1982.* This work was supported by grants from the National Science Foundation (PCM-77-25099 to R.R.B. and PCM-79-04607 to M.T.R.) and the National Institutes of Health (CA-23076 to R.R.B., EY-01483 to H.Y., and GM-23467 to M.T.R.).

‡ Present address: Proctor & Gamble, Ivorydale Technical Center, Cincinnati, OH 45217.

§ Present address: Envirogenics Systems, El Monte, CA 91731.

[1] Abbreviations: holo, RNA polymerase holoenzyme; core, core RNA polymerase; Tris, 2-amino-2-(hydroxymethyl)-1,3-propanediol; EDTA, ethylenediaminetetraacetic acid; Bicine, *N,N*-bis(2-hydroxyethyl)glycine; Hepes, *N*-(2-hydroxyethyl)piperazine-*N'*-2-ethanesulfonic acid; QLS, quasi-elastic light scattering.

0006-2960/82/0421-5539$01.25/0

species from the Svedberg equation. (QLS experiments on holoenzyme were not readily interpretable.) Determination of the sizes of the low salt oligomers allowed us to model the equilibria and calculate equilibrium constants as a function of salt concentration. The salt dependence of the equilibrium constants in the absence of Mg^{2+} is consistent with a cooperative effect of anions on the aggregation equilibria. A simple allosteric model provides a plausible molecular mechanism for this cooperative effect. Possible implications of these results for the DNA binding of RNA polymerase are briefly considered.

Materials and Methods

Reagents. All chemicals were reagent grade. All solutions were prepared with distilled water deionized by a Millipore Q3 water system.

Buffers. Storage buffer for the RNA polymerase consisted of 0.01 M Tris (pH 7.9 at 20 °C), 0.1 M NaCl, 10^{-4} M EDTA, 10^{-4} M dithiothreitol, and 50% (v/v) glycerol. The Mg^{2+}-free buffers used in this study contained 0.01 M Tris-HCl (pH 8.0 at 20 °C), 10^{-4} M EDTA, 2×10^{-3} M 2-mercaptoethanol, 3% (v/v) glycerol, and an appropriate amount of added NaCl. Buffers used to study the aggregation in the presence of Mg^{2+} contained 0.010 M $MgCl_2$ but were otherwise identical with the Mg^{2+}-free buffers. The buffers used to investigate the temperature dependence of the aggregation reactions contained Bicine rather than Tris. The pH studies used either cacodylate or Hepes as buffering agents.

RNA Polymerase. RNA polymerase (both core and holo) from the K12 strain of *E. coli* was prepared by the method of Burgess & Jendrisak (1975) as modified by Lowe et al. (1979). The σ content of the holoenzyme was estimated from densitometric tracings of Coomassie brilliant blue stained gels (Burgess, 1976) to be 87 ± 10%. Holoenzyme used to study the sedimentation as a function of sodium chloride was supplemented with purified σ (Lowe et al., 1979) to give a σ content of 140 ± 10%. The light-scattering experiments and the studies of the sedimentation of holoenzyme as a function of enzyme concentration at fixed salt conditions were performed with holo supplemented with σ to 115 ± 10%.

Triplicate measurements of the enzyme activities were performed on the single preparation of holoenzyme (87% σ saturated) and of core polymerase used in this investigation. The assay of Chamberlin et al. (1979) was used. T7 DNA was used as template. Using the elongation rate obtained from our plots of moles of cytosine triphosphate incorporated vs. time, we found our holoenzyme to be 66 ± 10% active and our core enzyme to be 43 ± 9% active. We found that the fraction of active core enzyme molecules was independent of the level of σ complementation in the range 60–75% saturation.

A partial specific volume of 0.738 mL/g was used for core polymerase, and a value of 0.742 mL/g was used for holoenzyme (Burgess, 1969). On the basis of a molecular weight of 3.85×10^5 for core polymerase (Burgess, 1976) and one of 7.0×10^4 for σ (Burton et al., 1981), a molecular weight of 4.55×10^5 was used for RNA polymerase holoenzyme. Protein concentrations were determined spectrophotometrically on a Gilford 2400-S by using $\epsilon_{280}^{1\%}$ values (corrected for light scattering) of 6.2 for holoenzyme and 5.5 for core polymerase (Burgess, 1976).

Sample Preparation. Samples used to study the salt dependence of the sedimentation of RNA polymerase were prepared by diluting an aliquot of the enzyme in storage buffer with another buffer to yield the desired sodium chloride concentrations. The protein concentration of each sample was measured. Concentrations of holoenzyme used in the experiments in Figure 6 ranged from 0.28 to 0.34 mg/mL. Core polymerase concentrations in the experiments summarized in Figure 1 varied from 0.25 to 0.33 mg/mL.

For the light-scattering measurements and the studies of the protein concentration dependence of the $\bar{s}_{20,w}$ at various fixed salt conditions, aliquots of polymerase in storage buffer were diluted with the dialysis buffer to yield a minimum volume of 1 mL of solution at a protein concentration somewhat higher than desired. The sample was then dialyzed twice against 1000 mL of the desired buffer for a total of 5–6 h at 4 °C.

Measurement of Densities and Viscosities. Relative densities of sample solutions or solvent were determined at room temperature to ±0.4% precision by weighing aliquots in 100- or 200-μL Dade micropipets. The micropipets were calibrated with water at the same temperature. The relative densities of samples and solvents were equal within experimental error in most cases. An Ubbelohde-style viscometer was used to measure the relative viscosities of the solvents. Measurements were made in a water bath controlled at 24.82 ± 0.03 °C. Solvent solutions were prepared in a manner analogous to that described above for preparation of samples by using an aliquot of storage buffer with no enzyme. The precision of our relative viscosity measurements is only ±1% due to the difficulty of precise volumetric transfer of the 50% glycerol storage buffer.

Sedimentation Velocity. (A) Experimental. Sedimentation velocity experiments were performed on a Beckman Model E analytical ultracentrifuge equipped with electronic speed control, RTIC unit, monochromater, and photoelectric scanner with multiplexer. Double-sector, 12-mm aluminum-filled Epon centerpieces were used. Scans were taken at 280 nm. Experiments on holoenzyme were performed at 28 000–32 000 rpm. Speeds for the core polymerase experiments varied from 18 000 to 32 000 rpm. Pressure effects were found to be negligible over this range of speeds (see below). All experiments were performed at approximately 20 °C. After initial prequilibration of the rotor and chamber to the desired temperature, the temperature was allowed to drift downward during the run. The maximum drift in any of these experiments was 0.4 °C. A drift of 0.2 °C or less was recorded for most of the runs.

(B) Pressure Effects. The pressure gradient that is established within a cell containing an interacting system and undergoing sedimentation at high angular velocities may have a dramatic influence on the sedimentation behavior observed, if a large molar volume change accompanies the reaction (TenEyck & Kauzmann, 1967; Kegeles et al., 1967; Josephs & Harrington, 1968; Harrington & Kegeles, 1973). Two types of experiments were performed to test whether our results for the aggregation of core and holo polymerase in the presence of Mg^{2+} were complicated by measurable pressure effects on the equilibrium constants. In one type of experiment, the hydrostatic pressure over the protein solution was varied by layering mineral oil over the sample (Josephs & Harrington, 1968). In a second test for pressure effects, a protein sample was sedimented first at 14 000 rpm, mixed, and then resedimented at 32 000 rpm, or vice versa. We could detect no pressure effect on our measured values of the $\bar{s}_{20,w}$. However, our experimental uncertainty (±3.3%) at the conditions used could mask a molar volume change as large as 0.4 ± 0.1 L/mol of core octamer or 0.8 ± 0.3 L/mol of holo dimer.

(C) Data Analysis. Sedimentation coefficients were obtained by using equivalent-boundary positions (Goldberg, 1953). This type of analysis, though more laborious than the standard "midpoint" analysis, is necessary when dealing with

an associating or dissociating system because it yields the weight-average sedimentation coefficient for the sample. The boundaries were digitized by using a Tektronix 6954 graphics tablet. At least 20 points per scan were acquired as input to the integration routine used to calculate the equivalent-boundary position, $\bar{r}$. Observed sedimentation coefficients were corrected to standard conditions (water at 20 °C) by using the measured relative densities and viscosities. The ratio of the 95% confidence limit of the slope of ln $\bar{r}$ vs. time to that slope was used as the fractional error of the sedimentation coefficient.

Analysis of the holoenzyme data requires further comment. In studying the sedimentation of holoenzyme at any fixed set of solution conditions, the molar ratio of σ to core critically affects the $\bar{s}_{20,w}$ measured (Berg & Chamberlin, 1970). We have chosen to eliminate the problems due to the presence of core polymerase aggregates at the low salt extreme by using holoenzyme complemented with σ to 140 ± 10% saturation. The presence of excess σ can be seen as a small (~6% of the total absorbance), slow-sedimenting boundary trailing the main boundary. The $s_{20,w}$ of this component was estimated to be 6 ± 3 S. The error in this estimate is large as a result of the small size of the σ boundary; however, it is in reasonable agreement with the value of ~5 S obtained by glycerol gradient centrifugation (Burgess et al., 1969). The height of the σ plateau was then used as the base line for the holoenzyme boundary.

Quasi-elastic Light Scattering. (*A*) *Experimental.* Diffusion coefficients were measured by quasi-elastic light scattering by using the 514.5-nm line of an argon ion laser (Lexel Model 75-.2) in the homodyne mode of detection (Berne & Pecora, 1976). A laser power of approximately 50 mW was used in these experiments. Each sample was filtered directly into the scattering cell through a 0.45-μm cellulose acetate filter (Millipore HA). Protein loss upon filtration was found to be minimal. The scattering cell was placed in a refractive index matching bath mounted on a goniometer table (Malvern RR103). Scattered light was collected by a photomultiplier tube (ITT, Model FW 130). The output photocount was sent to a real-time autocorrelator (64-channel multibit, Malvern K7025) interfaced to a microcomputer (Apple II, Apple Computer Co., Cupertino, CA). The accumulated autocorrelations of the photocounts were initially analyzed on the microcomputer and subsequently transferred to a Harris/7 computer for detailed analysis. The instrument has been calibrated with several standards (Amis, 1981).

(*B*) *Data Analysis.* The decay constant, Γ, for the autocorrelation function of the scattered photocount has been obtained by fitting the experimental data to either a single exponential decay or a cumulant expansion (Koppel, 1972). The diffusion coefficient, D, is related to Γ through the scattering wave vector, κ^2, such that $\Gamma = D\kappa^2$. Here, κ is defined by $(4\pi n/\lambda_0) \sin(\theta/2)$, where n is the refractive index of the scattering medium, λ_0 is the in vacuo incident wavelength, and θ is the scattering angle. For a polydisperse collection of scattering particles, a z-average diffusion coefficient is obtained (Berne & Pecora, 1976). In principle, the translational diffusion coefficient may be calculated from the value of Γ at a single scattering angle. In practice, it is preferrable to measure Γ for a number of scattering angles and to evaluate D from the slope of Γ vs. κ^2. We report diffusion coefficients for core polymerase based on data collected at 10–12 scattering angles. Uncertainties reported are the 95% confidence limit of the slope obtained by using the Student's t distribution. Observed diffusion coefficients were corrected to standard conditions by using the measured relative viscosities.

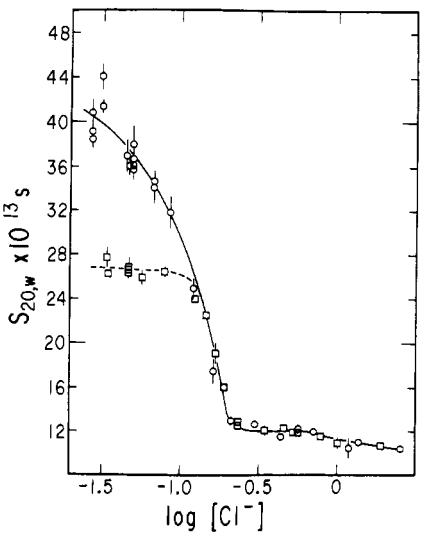

FIGURE 1: Dependence of the $\bar{s}_{20,w}$ of core polymerase on [Cl$^-$] in the presence (○) and absence (□) of 0.01 M $MgCl_2$. Sedimentation was performed at 20 °C at speeds ranging from 18 000 to 32 000 rpm. Core concentrations used were ~0.29 mg/mL.

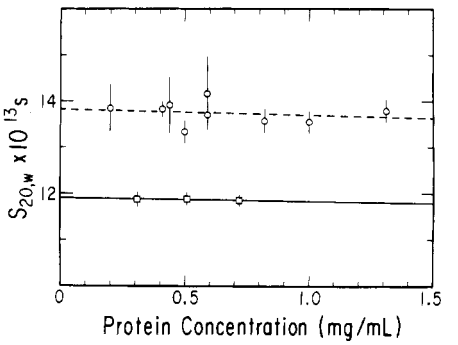

FIGURE 2: Dependence of the $\bar{s}_{20,w}$ of holo (○) and core (□) monomers on the total protein concentration. The lines through the data are the linear least-squares fits. The holo data were obtained at 0.40 M NaCl (in the absence of $MgCl_2$) on a sample which was supplemented to 115 ● 10% σ. The core measurements were made in 0.53 M NaCl (in the absence of $MgCl_2$).

In situations where Γ is observed to depend on scattering angle (as is the case for holoenzyme in this work), one may conclude that the scattering sample is polydisperse or that more than one significant relaxation process exists. In such instances, it is frequently impossible to extract any detailed, physically meaningful information about the scattering population from the data (Brehm & Bloomfield, 1975; Bloomfield & Lim, 1978).

Results

Core RNA Polymerase. (*A*) *At High Salt, Core Exists as a Monomer in the Presence or Absence of* Mg^{2+}. The weight-average sedimentation coefficients (corrected to standard conditions) of core RNA polymerase in NaCl with and without 0.01 M $MgCl_2$ are presented as a function of chloride concentration in Figure 1. At chloride concentrations between 0.25 M (log [Cl$^-$] = −0.60) and 0.8 M (log [Cl$^-$] = −0.10), core polymerase sediments as a monomeric species in the presence or absence of 0.01 M $MgCl_2$. The presence of a single nonreacting species was confirmed by the weak dependence of the $\bar{s}_{20,w}$ on protein concentration shown in Figure 2. The concentration dependence follows the standard equation $\bar{s}_{20,w} = s^0_{20,w}(1 - gc)$ where c is the protein concen-

Table I: Summary of Light-Scattering and Sedimentation Data for Core RNA Polymerase

solution conditions	core concn (mg/mL)	$\bar{D}_{20,w} \times 10^7$ (cm²/s)	$\bar{s}_{20,w} \times 10^{13}$ (S)	M (g/mol)
(I) 0.40 M NaCl, no Mg^{2+}	0.52	2.87 ± 0.09	11.9 ± 0.2	(3.85 ± 0.17) × 10^5
(II) 0.40 M NaCl, 0.01 M $MgCl_2$	0.52	2.65 ± 0.08	*b*	(4.17 ± 0.18) × 10^5 [a]
(III) 1.16 M NaCl, 0.01 M $MgCl_2$	0.39	2.4 ± 0.2	10.4 ± 1.0	(4.0 ± 0.7) × 10^5
(IV) 0.027 M NaCl, no Mg^{2+}	0.84	1.83 ± 0.03	26.7 ± 0.3	(1.36 ± 0.04) × 10^6
(V) 0.016 M NaCl, no Mg^{2+}, 9% (v/v) glycerol	0.92	1.82 ± 0.06	25.8 ± 0.4	(1.33 ± 0.07) × 10^6
(VI) no NaCl, 0.01 M $MgCl_2$	0.93	1.40 ± 0.04	44.5 ± 2.8	(3.0 ± 0.3) × 10^6
	0.56	1.43 ± 0.02	42.0 ± 1.0	(2.7 ± 0.1) × 10^6
	0.55	1.45 ± 0.04	41.7 ± 0.8	(2.7 ± 0.1) × 10^6
	0.39	1.46 ± 0.03	42.0 ± 1.0	(2.7 ± 0.1) × 10^6
	0.26	1.47 ± 0.03	38.8 ± 1.0	(2.5 ± 0.1) × 10^6

[a] Calculated assuming $\bar{s}_{20,w} = 11.9 \pm 0.2$ S. [b] Not measured.

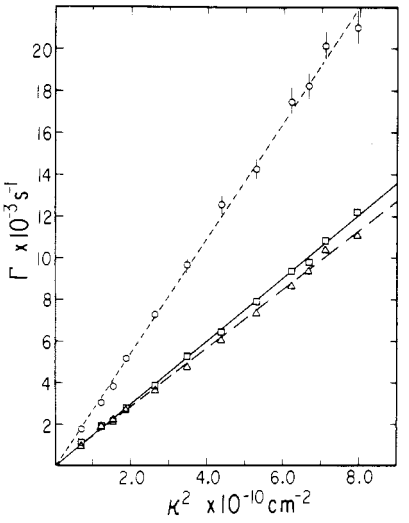

FIGURE 3: Dependence of the decay constant of the autocorrelation function (Γ) on the scattering vector (κ^2). Data are presented for core monomer [(○) 0.4 M NaCl, no $MgCl_2$; 0.53 mg/mL core), core tetramer [(□) 0.034 M NaCl, no $MgCl_2$; 0.84 mg/mL core), and core octamer (△) 0.01 M $MgCl_2$, no NaCl; 0.93 mg/mL core). Values of Γ are from a single exponential fit to the autocorrelation data. For the core monomer and octamer, Γ has also been obtained by fitting the autocorrelation data with a cumulant expansion. The values of Γ at each scattering angle obtained from these two fitting procedures were identical within the statistical precision of the measurement. The lines through the data are the linear least-squares fits. The slopes of these lines are the diffusion coefficients (not corrected to standard conditions) of the samples (see Materials and Methods).

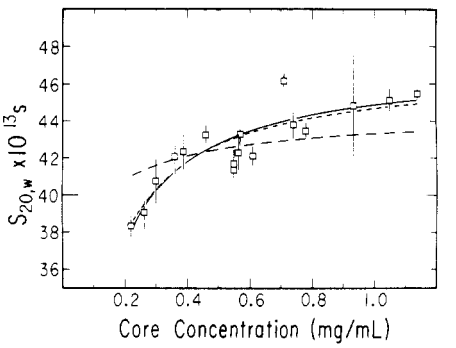

FIGURE 4: Dependence on protein concentration of the $\bar{s}_{20,w}$ of core polymerase in 0.01 M $MgCl_2$ with no added NaCl. The theoretical fits obtained assuming an isodesmic association to an octamer (– –), a monomer–tetramer–octamer stoichiometry (- - -), and a monomer–octamer scheme (—) are presented with the experimental data.

tration in milligrams per milliliter and g is the hydrodynamic nonideality constant for the species. The sedimentation coefficient of this species extrapolated to infinite dilution, $s^0_{20,w}$, is 11.9 ± 0.2 S. The hydrodynamic nonideality constant is (7 ± 3) × 10^{-3} mL/mg, a typical value for a nonassociating system (Teller, 1973).

The diffusion coefficient of core polymerase was measured at several high salt conditions (see Table I, entries I and II, and Figure 3). The average value for the $\bar{D}_{20,w}$ at 0.40 M NaCl is (2.76 ± 0.11) × 10^{-7} cm²/s. When combined in the Svedberg equation (Schachman, 1959) with the measured $s^0_{20,w}$ (11.9 ± 0.2 S), a molecular weight of (4.0 ± 0.2) × 10^5 is obtained. This is in agreement with the commonly accepted molecular weight for the core monomer (Burgess, 1976). Diffusion coefficients measured in the presence of Mg^{2+}, (2.65 ± 0.08) × 10^{-7} cm²/s, and absence of Mg^{2+}, (2.87 ± 0.09) × 10^{-7} cm²/s, differ by somewhat more than experimental uncertainty. If this difference is real, it suggests that the binding of Mg^{2+} to the core polymerase may induce a conformational change in the protein. The invariance of the molecular weight of core enzyme between 0.4 and 1.16 M NaCl (as calculated from $\bar{D}_{20,w}$ and $\bar{s}_{20,w}$; see Table I, entries I–III) suggests that the gradual reduction in the $\bar{s}_{20,w}$ observed at concentrations greater than 0.80 M Cl^- is due to changes in the frictional coefficient of the monomer rather than dissociation of the core enzyme into its subunits.

(B) At Low Salt, Core Polymerase Aggregates to an Octamer in the Presence of Mg^{2+}. In Figure 1, it can be seen that the $\bar{s}_{20,w}$ of core polymerase increases to over 40 S as the sodium chloride concentration is reduced in the presence of 0.01 M $MgCl_2$. The behavior of the $\bar{s}_{20,w}$ with decreasing salt is qualitatively similar to that observed by Berg & Chamberlin (1970) in 0.01 M $MgCl_2$ when $(NH_4)_2SO_4$ was used to vary the ionic strength.

With no NaCl added to the buffer, both the $\bar{s}_{20,w}$ (Figure 4) and $\bar{D}_{20,w}$ (Table I, entry VI) show a dependence on the protein concentration. The positive dependence of the $\bar{s}_{20,w}$ on core concentration indicates the existence of a reversible aggregation equilibrium; smaller species (monomer or intermediates) must exist in equilibrium with the largest aggregate. Apparent average molecular weights[2] were calculated from the values of $\bar{s}_{20,w}$ and $\bar{D}_{20,w}$ for the protein concentrations at which both types of experiments were performed (see the final column of entry VI of Table I). The ratio of these molecular weights to the monomer molecular weight (3.85 × 10^5) increases from 6.5 to 7.8 as the protein concentration increases from 0.26 to 0.93 mg/mL. This trend in molecular weight strongly suggests that the largest aggregate formed is an octamer. If s is assumed proportional to $M^{2/3}$, the relationship which holds for a series of solid particles of identical f/f_0 (the ratio of the frictional coefficient of the actual particle to that of an unhydrated sphere with the same partial specific volume

[2] The type of average molecular weight obtained from the Svedberg equation for a heterogeneous mixture when a weight-average $\bar{s}_{20,w}$ and a z-average $\bar{D}_{20,w}$ are used does not correspond to any of the typical molecular weight averages (Schachman, 1959).

and molecular weight; Schachman, 1959), an octamer of an 11.9 S monomer should have an $s^0_{20,w}$ of 47.6 S. Calculation of the diffusion coefficient for the octamer with this $s^0_{20,w}$ yields a value of 1.40×10^{-7} cm^2/s in agreement with the $\bar{D}_{20,w}$ measured at the largest protein concentration used [$(1.40 \pm 0.04) \times 10^{-7}$ cm^2/s]. At this protein concentration, the agreement at each scattering angle of the decay constants obtained by fitting the autocorrelation data to either a single exponential (Figure 3) or a cumulant expansion supports the view that the z-average $\bar{D}_{20,w}$ measured under these conditions has only minimal contributions from species smaller than the largest aggregate. The apparent average molecular weight calculated at that protein concentration is less than 8 times the monomer molecular weight because the value of the $\bar{s}_{20,w}$, a weight-average quantity, would be more sensitive to the existence of any smaller species in the sample.

(*C*) *At Low Salt in the Absence of Mg^{2+}, Core Polymerase Aggregates to a Tetramer.* In the absence of Mg^{2+} the sedimentation coefficient of core polymerase reaches an apparent plateau at a value of 26.7 ± 0.5 S below 0.1 M Cl^- (Figure 1). The dependence of the $\bar{s}_{20,w}$ on protein concentration (for concentrations greater than 0.33 mg/mL) at 0.034 M Cl^- (log $[Cl^-] = -1.47$) is linear (data not shown); from the protein concentration dependence one obtains $s^0_{20,w} = 28.1 \pm 0.2$ S and $g = (6 \pm 1) \times 10^{-2}$ mL/mg. The dependence of the sedimentation coefficient of core polymerase on protein concentration was also examined between 0.18 and 0.63 mg/mL at 0.047 M Cl^- (log $[Cl^-] = -1.33$). Below 0.25 mg/mL core the $\bar{s}_{20,w}$ decreases (data not shown), indicating the presence of a reversible aggregation equilibrium involving the monomer and any intermediates. From the data at 0.034 M Cl^- the $s^0_{20,w}$ of the largest core polymerase aggregate formed in the absence of Mg^{2+} must be at least 28.1 S. It is probably larger because the data obtained at lower core concentrations (and slightly higher salt) indicate that smaller species are in equilibrium with the largest aggregate.

A $\bar{D}_{20,w}$ of $(1.82 \pm 0.06) \times 10^{-7}$ cm^2/s was obtained on two separate scattering samples of core polymerase at low salt (see Table I, entries IV and V, and Figure 3). The average molecular weights calculated are approximately 3.4–3.5 times the monomer molecular weight. If the aggregation were complete under these solution conditions, this would indicate that the aggregate is either a trimer or a tetramer. The dependence of the weight-average sedimentation coefficients upon core concentration at these salt concentrations indicates that the largest aggregate exists in equilibrium with some smaller species. The calculated apparent molecular weight is consistent with a tetrameric species in equilibrium with smaller units. It seems reasonable to assume that the z-average $\bar{D}_{20,w}$ measured under these conditions is approximately that of the largest scattering species. If this is the case, we calculate, using the Svedberg equation, that the $s^0_{20,w}$ of the tetramer is 30.1 S. This is identical with the predicted value of the sedimentation coefficient of a tetramer of an 11.9 S monomer if the $M^{2/3}$ power dependence of the $s^0_{20,w}$ is assumed (Schachman, 1959).

(*D*) *The Observed Salt Dependence of the $\bar{s}_{20,w}$ of Core Polymerase Is Highly Sensitive to the Identity of the Monovalent Anion but Is Comparatively Insensitive to the Identity of the Monovalent Cation.* The effect of variation of the salt type on the sedimentation coefficient of core RNA polymerase in the absence of Mg^{2+} is presented Figure 5. The data obtained in NH_4Cl or NaCl are found to lie on the same curve. This is in agreement with earlier observations that the sedimentation of polymerase is comparatively insensitive to

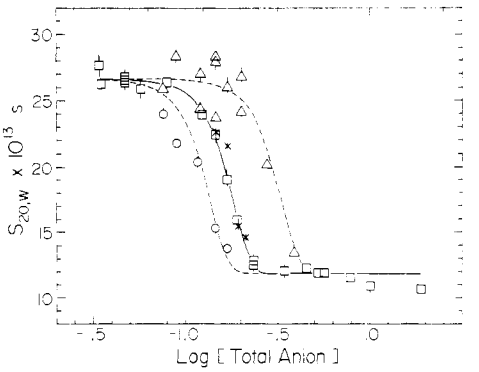

FIGURE 5: Effects of NaI (○), NaCl (□), NH_4Cl (×), and NaF (△) on of the $\bar{s}_{20,w}$ of core polymerase in the absence of $MgCl_2$. The lines drawn through the data points are theoretical predictions of the $\bar{s}_{20,w}$ by using eq 3 as described under Results.

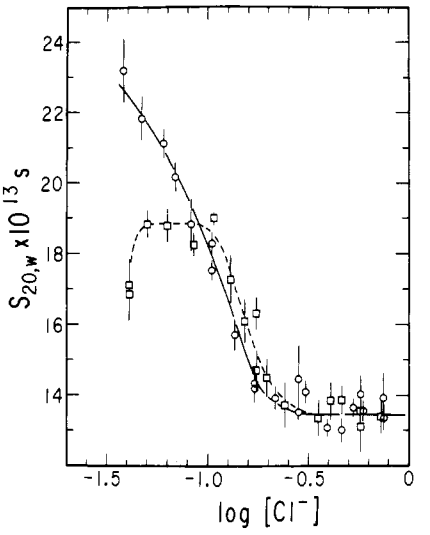

FIGURE 6: Dependence of the $\bar{s}_{20,w}$ of holoenzyme on the concentration of total chloride in the presence (○) and absence (□) of 0.01 M $MgCl_2$. Sedimentation was performed at 28 000–32 000 rpm at 20 °C. Holo concentrations were ~0.31 mg/mL. The holoenzyme used was 140% σ saturated.

changes in the univalent cation (Stevens et al., 1966; Beabealashvilly & Savotchkina, 1973). On the other hand NaI shifts the aggregation curve to lower anion concentrations while NaF shifts the aggregation curve to higher anion concentrations. We conclude from these data that the appropriate variable to use in presenting our results is the logarithm of the total anion concentration of the buffer (including contributions from $MgCl_2$ and Tris-HCl); in general, the anion used was Cl^-.

RNA Polymerase Holoenzyme. (*A*) *At High Salt, the Sedimentation Behavior of Holoenzyme Indicates the Presence of a Single, Nonreacting Species While the Light-Scattering Experiments Indicate Possible Heterogeneity.* In Figure 6 it can be seen that holoenzyme (complemented with σ to 140 ± 10% saturation) sediments at 13.5 ± 0.6 S above 0.20 M Cl^- (log $[Cl^-] = -0.70$) in the presence and absence of $MgCl_2$. The most probable cause of the decreased precision of the values of the $\bar{s}_{20,w}$ for holoenzyme (~5% vs. ~3% for core enzyme) and possibly the greater scatter in values obtained at high chloride concentrations is the need to subtract the boundary of the excess σ (see Materials and Methods). The presence of a single, nonreacting sedimenting species at high salt was verified at 0.40 M NaCl with no $MgCl_2$ in the buffer by using a sample of holoenzyme complemented with σ to 115 ± 10%. These data, presented in Figure 2, yield a value of

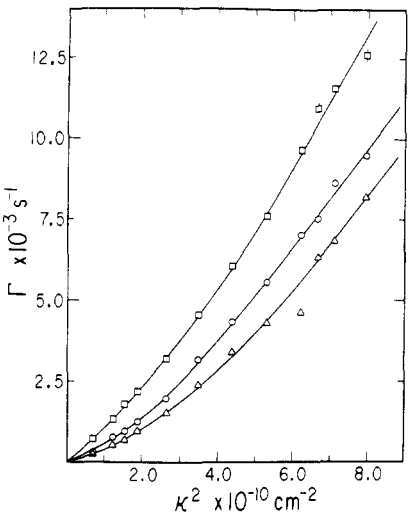

FIGURE 7: Dependence of Γ on κ^2 for holo RNA polymerase. Data taken at 0.4 M NaCl with no $MgCl_2$ (□), 0.04 M NaCl with 0.01 M $MgCl_2$ (△), and 0.04 M NaCl without $MgCl_2$ (○) are presented. The values of Γ were obtained by fitting a cumulant expansion to the autocorrelation data. The data are corrected to standard conditions.

$s^0_{20,w}$ = 13.7 ± 0.2 S and g = (5 ± 2) × 10^{-3} mL/mg.

When holoenzyme at a concentration of 0.6 mg/mL was examined by quasi-elastic light scattering in 0.4 M NaCl with or without $MgCl_2$, a plot of Γ vs. κ^2 appeared linear (data not shown). The $\bar{D}_{20,w}$ for these two samples was (1.98 ± 0.07) × 10^{-7} cm^2/s while the $\bar{s}_{20,w}$ was 14.1 ± 0.5 S. These values, when inserted into the Svedberg equation, yield an apparent average molecular weight of (6.6 ± 0.5) × 10^5. The commonly accepted range for the molecular weight of holoenzyme monomer is (4.6–5.0) × 10^5. Under these same salt conditions but at a higher protein concentration (1.3 mg/mL holo), curvature appears in a plot of Γ vs. κ^2 (Figure 7). The apparent molecular weight obtained by using the decay constant at a scattering angle of 120° to calculate an apparent diffusion coefficient is (7.5 ± 0.3) × 10^5, while that obtained by using the apparent diffusion coefficient at 30° is (1.3 ± 0.3) × 10^6. These results at two different concentrations of holo suggest the presence of a concentration-dependent aggregation process. However, the sample heterogeneity indicated by the light-scattering data at high salt seems inconsistent with the weak dependence of the sedimentation coefficient upon holo concentration shown in Figure 2.

(B) At Low Salt Holoenzyme Aggregates in the Presence or Absence of Mg^{2+}. In the presence of Mg^{2+}, the $\bar{s}_{20,w}$ of holoenzyme rises continuously with decreasing concentration of added NaCl (Figure 6). A sedimentation coefficient of 23.2 ± 0.9 S is obtained at 0.038 M Cl^- (log [Cl^-] = −1.42), the lowest salt concentration examined. The observed dependence of the $\bar{s}_{20,w}$ on electrolyte concentration is similar to that observed previously for holoenzyme by Berg & Chamberlin (1970).

In the absence of Mg^{2+}, between 0.11 M (log [Cl^-] = −0.96) and 0.05 M Cl^- (log [Cl^-] = −1.30), the $\bar{S}_{20,w}$ of holoenzyme reaches a maximum value of 18.8 ± 0.4 S. The drop in $\bar{s}_{20,w}$ observed below 0.05 M Cl^- may be due to the primary charge effect (Schachman, 1959), though neither core polymerase nor holoenzyme in 0.01 M $MgCl_2$ shows a comparable effect (see Discussion).

The QLS experiments on holoenzyme (~0.5 mg/mL) at 0.04 M NaCl with or without the presence of Mg^{2+} revealed a marked angular dependence of the decay constant of the autocorrelation function (Figure 7). To illustrate the potential degree of sample heterogeneity indicated by the QLS results in the absence of Mg^{2+}, we have used the $\bar{s}_{20,w}$ of the sample to calculate apparent molecular weights from the $\bar{D}_{20,w}$'s obtained at the smallest and largest scattering angles investigated. We calculate an apparent molecular weight of (1.5 ± 0.1) × 10^6 from the $\bar{D}_{20,w}$ at 120° and an apparent molecular weight of (4.4 ± 0.3) × 10^6 from the $\bar{D}_{20,w}$ at 30°. Similar results were obtained for the sample containing Mg^{2+}. We are unsure of the cause of this apparent heterogeneity (see Discussion).

We are consequently unable to specify the stoichiometries of the aggregates of holoenzyme. However, Pilz et al. (1972) used the absolute intensities measured in their small-angle X-ray scattering experiments on holoenzyme to determine that the low salt species in the presence of Mg^{2+} was a dimer of the high salt species. If the 13.7 ± 0.2 S species we observe at high salt is the monomer, then a dimer would be predicted (assuming that $s \propto M^{2/3}$) to possess a sedimentation coefficient of 21.8 ± 0.5 S. This value is in reasonably close agreement with the sedimentation coefficients we measure at the lowest concentrations of Cl^- in the presence of Mg^{2+}. The value measured at 0.038 M (23.2 ± 0.9 S) is somewhat greater than this; however, the error in the measurement is sufficiently large to overlap at the low end of its uncertainty with the predicted value. Additionally, if a small fraction of core polymerase is present (in spite of the excess σ), the weight-average $\bar{s}_{20,w}$ would be larger than expected. For purposes of calculating equilibrium constants from our sedimentation data, we have assumed that a dimerization takes place.

Calculation and Analysis of Equilibrium Constants for Aggregation. (A) General Theory. We have calculated equilibrium constants for the aggregation equilibria of RNA polymerase core and holoenzyme by assuming a simple monomer–j-mer association scheme. The assumed absence of intermediates allows the equilibrium constant to be calculated from the weight-average sedimentation coefficient obtained at a single total protein concentration (C_{tot}) if the sedimentation coefficients of the monomer (s^0_1) and j-mer (s^0_j) are known (Fugjita, 1975). The concentrations of the monomer C_1) and j-mer (C_j) needed for calculation of the equilibrium constants are obtained from the simultaneous solution of the equation defining the weight-average sedimentation coefficient, $\bar{s}_{20,w} = (C_1 s^0_1 + C_j S^0_j)/C_{tot}$ and $C_{tot} = C_1 + C_j$. The small concentration dependences of the monomer and j-mer sedimentation coefficients arising from the hydrodynamic nonideality of the protein solution were neglected in performing these calculations.

If a ligand binds to different extents to the reactant and product species in a macromolecular reaction, the equilibrium extent of that reaction will shift as a function of the concentration of the ligand. Binding polynomials (Wyman, 1964; Schellman, 1975; Record et al., 1978; Hess & Szabo, 1979) and the preferential interaction parameter (Eisenberg, 1976; Schellman, 1978; Gekko & Timasheff, 1981a,b) have both been used extensively to analyze such effects upon the observed equilibrium constants. For reactions such as those investigated here in which the evidence points to a site-binding effect rather than a preferential solvation effect (see Discussion), the binding polynomial formulation is typically preferred.

The reaction of interest is the aggregation of j protomers (P) to form an aggregate (A):

$$jP \overset{K_{obsd}}{\rightleftharpoons} A$$

The observed equilibrium constant may be written as

$$K_{obsd} = \frac{[A]}{[P]^j} = K^0 \frac{\Sigma_A}{(\Sigma_P)^j} \qquad (1)$$

where K^0 represents the value of the equilibrium constant in the limit of low electrolyte concentration (i.e., no anion binding) and $\sum_m$ is the binding polynomial of species m. [In this analysis we assume that the ratio of the activity coefficient of the aggregate to that of the protomers (raised to the power j) is independent of ligand concentration and that the ligand concentration is sufficiently low to neglect ligand effects on water activity.]

The ligand we have used is the anion X^-. In general, separation of an electrolyte effect into contributions from the cation and anion may not be readily effected (Record et al., 1978). However, the experimental evidence (Figure 5) that different cations do not appreciably affect our observed $\bar{s}_{20,w}$ at a given electrolyte (and protein) concentration while different anions do implies that in this case we may identify the observed effect as an anion effect. In analyzing the dependence of K_{obsd} on anion concentration we have considered two different physical models for the role of the anions in the aggregation equilibrium. Since the anion binding polynomials for these models are different, each model predicts a characteristic dependence of K_{obsd} on anion concentration. (Our data show that aggregation is favored by reduction of the anion concentration; therefore, both models must be formulated such that the j monomers bind more anions individually than they do when combined within the aggregate.)

(*1*) *Independent, Identical Sites Model.* The first model considered is one in which a class of n_1 independent, identical anion binding sites with affinity constant k_1 available on each monomer is occluded upon aggregation. In this case, the binding polynomials are $\sum_A = 1$ (no available anion binding sites) and $\sum_P = (1 + k_1[X^-])^{n_1}$. (In this and subsequent models, it is recognized that other anion binding sites that are not affected by aggregation may exist on the protomers. It is assumed that the contribution from these sites to the binding polynomials are factorable from the contribution of the relevant sites and that, once factored out, they will cancel in the binding polynomial ratio of eq 1.) For the independent, identical site model, the dependence of K_{obsd} on $[X^-]$ is given by

$$\log K_{obsd} = \log K^0 - jn_1 \log (1 + k_1[X^-]) \qquad (2)$$

(*2*) *Completely Cooperative Model.* The second model considered is one in which a class of n_2 sites which bind anions in a completely cooperative manner is lost from each of the j monomers upon aggregation. In this case, the binding polynomials are $\sum_A = 1$ and $\sum_P = (1 + k_2[X^-]^{n_2})$ where k_2 is the equilibrium constant for the cooperative binding of the n_2 anions to the protomer (in units of M^{-n_2}). Therefore, for the completely cooperative model of anion binding, the equilibrium constant for aggregation is given by

$$\log K_{obsd} = \log K^0 - j \log (1 + k_2[X^-]^{n_2}) \qquad (3)$$

At sufficiently high anion concentrations, these models reduce to the same form. In this limit (saturation of sites), log K_{obsd} will be linear in log $[X^-]$. The negative of the slope in this region, $-(\mathrm{d} \log K_{obsd}/\mathrm{d} \log [X^-])$, yields the maximum amount of anion release for the reaction.

(*B*) *Is It Reasonable To Neglect Intermediates in the Calculation of Equilibrium Constants for Core Octamer and Tetramer Formation*? The appropriateness of the use of the monomer–j-mer stoichiometry was checked for core octamer formation by fitting sedimentation data obtained as a function of core concentration to several alternative aggregation schemes. The following schemes were considered: (1) a monomer–octamer stoichiometry, (2) a model involving a tetrameric intermediate, and (3) isodesmic association (with j varied from 2 to 16), for which the free energy increment for the addition of each monomer to the growing aggregate is assumed to be the same (van Holde, 1975; Holloway & Cox, 1974). The data were fit to each of the three models by using a least-squares method. Relative goodness of fit was judged by comparing the sum of the squares of the deviations. The (infinite dilution) sedimentation coefficient of the monomer (s^0_1) was taken to be 11.9 ± 0.2 S. Sedimentation coefficients of oligomers were calculated from s^0_1 by assuming that sedimentation coefficients are proportional to $M^{2/3}$ (Schachman, 1959).

Figure 4 compares the experimental dependence of the $\bar{s}_{20,w}$ on core concentration with the theoretical predictions of the three association schemes. The quality of the fit to the data obtained assuming an isodesmic association was poor for j = 8 (shown in Figure 4). A fit of comparable quality to that obtained for the monomer–octamer equilibrium and the monomer–tetramer–octamer scheme was obtained for the isodesmic scheme with j = 10 (not shown). The quality of the fit obtained by assuming an isodesmic association deteriorated as the value of j was increased above 10, ruling out the possibility of an indefinite self-association. Because we have determined that the molecular weight at low salt concentration approaches the molecular weight of an octamer with increasing concentrations of core and also because of the rarity of protein complexes composed of ten subunits (Klotz et al., 1975), we believe that the good fit achieved for the isodesmic 10-mer is accidental. The overall equilibrium constant for the formation of octamers obtained by the monomer–tetramer–octamer scheme [log K_8 (M^{-7}) = 48.0 ± 0.8] agreed closely with that calculated by using the monomer–octamer scheme [log K_8 (M^{-7}) = 47.3 ± 0.4]. Although this comparison does not eliminate the possibility that intermediates are important in the aggregation pathway, it suggests that it is not unreasonable to ignore the presence of intermediates in parameterizing this aggregation equilibrium.

We attempted similar fits with our data on the dependence of the $\bar{s}_{20,w}$ on protein concentration for the formation of tetramers (0.047 M Cl^- in the absence of Mg^{2+}). We were unable to obtain a reasonable fit with the two-parameter monomer–dimer–tetramer scheme when the $\bar{s}_{20,w}$ of the tetramer was set equal to 30 S. The two one-parameter models, (i) a monomer–tetramer stoichiometry and (ii) an isodesmic association with n = 4, yielded values for the log of the overall equilibrium constant for tetramer formation of 20.6 ± 0.4 and 22.7 ± 0.9, respectively (with K_4 in units of M^{-3}). The isodesmic model provides only a marginally better fit to the data than does the monomer–tetramer model.

(*C*) *Formation of Core Aggregates Is Accompanied by Substantial Anion Release; Tetramer Formation in the Absence of Mg^{2+} Appears To Involve a Cooperative Release of Anions from the Individual Monomers.* The chloride dependence of the equilibrium constants for core tetramer formation (no Mg^{2+}) is presented in Figure 8. The solid curve through the data points represents the weighted nonlinear least-squares fit to the completely cooperative model (eq 3). This fit is summarized by

$$\log K_4 (M^{-3}) = (20.5 \pm 0.2) - 4 \log (1 + k_2[Cl^-]^{4.2\pm0.2}) \qquad (4)$$

with log k_2 = 3.63 ± 0.04. (The error presented for each of the parameters represents the 95% joint parameter confidence interval for the fit.)

When the data were fit to the model with independent, identical sites, large values of n_1 (>10^2) and small values of k_1 (<0.1 M^{-1}) were required to reproduce the curvature of the

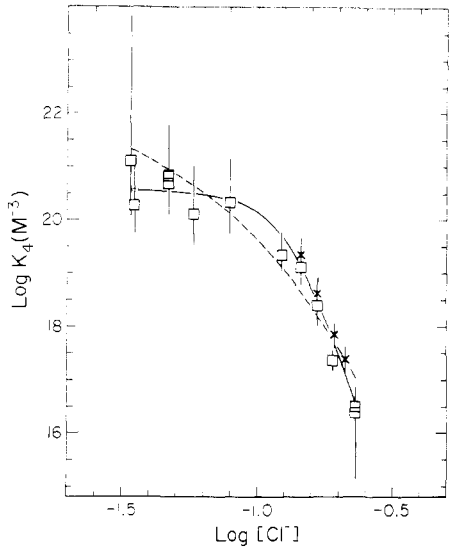

FIGURE 8: Dependence of the observed equilibrium constants for core tetramer formation on [Cl⁻]. The data were obtained by using either NaCl (□) or NH_4Cl (×) as the salt. The solid line through the data points is a theoretical best fit to the completely cooperative model; the dotted line represents the best fit to a model in which anions bind to independent, identical binding sites (n_1 = 4.2).

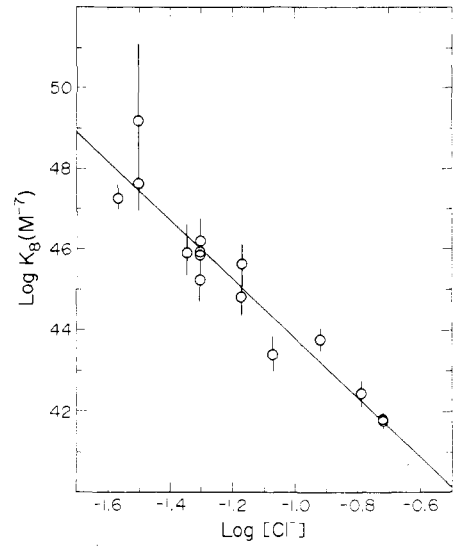

FIGURE 9: Dependence of the observed equilibrium constants for core octamer formation on [Cl⁻]. The linear least-squares fit line is drawn through the data.

data (Figure 8). This result (large n, small k) is more consistent with an effect of salt resulting from weak preferential interactions rather than one resulting from actual physical binding [see Schellman (1978)]. However, the observation of a specific anion effect on a negatively charged protein at relatively low electrolyte concentrations argues against such an explanation of the observed dependence of log K_4 on salt concentration. When n_1 is constrained to a fixed value consistent with physical binding, we obtain fits similar to the dashed line in Figure 8. The equation for this line (n_1 = 4.2) is log K_4 (M^{-3}) = (22.4 ± 0.1) − 4(4.2) log [1 + (4.7 ± 0.2)[Cl⁻]]. Although this curve does pass within the estimated uncertainties of most of the data points, the fit is significantly inferior to that provided by the completely cooperative model.

The chloride dependence of the equilibrium constants for octamer formation by core polymerase (with Mg^{2+}) is presented in Figure 9. Log K_8 appears linear in log [Cl⁻] over the entire range of [Cl⁻] examined. In the absence of curvature, it is impossible to extract any information concerning the molecular mechanism resulting in the anion release; one can, however, obtain the average number of anions released upon octamer formation in the [Cl⁻] range investigated from the slope of the line through the data. This line is described by

$$\log K_8\ (M^{-7}) = (36.4 \pm 1.3) - (7.3 \pm 1.4) \log [Cl^-] \quad (5)$$

for log [Cl⁻] < −0.70 ([Cl⁻] < 0.20 M). From the slope, we find that 0.9 ± 0.2 anion is released per monomer upon aggregation in this [Cl⁻] range. To allow a direct comparison of this result to that obtained in the absence of Mg^{2+}, we have obtained the linear least-squares fit to the region of Figure 8 in which log K_4 is apparently linear in log [Cl⁻]. The equation for this fit is log K_4 (M^{-3}) = (8.0 ± 0.5) − (13.5 ± 0.2) log [Cl⁻] for −0.84 < log [Cl⁻] < −0.64 (0.14 M < [Cl⁻] < 0.23 M). The slope indicates that 3.4 ± 0.1 anions are released per monomer upon tetramer formation in this range of salt concentrations.

(D) Holoenzyme Dimerization Is Also Accompanied by Substantial Anion Release; the Dimerization in the Absence of Mg^{2+} Is Most Readily Fit by a Model in Which Anion Binding to the Individual Monomers Is Cooperative. The

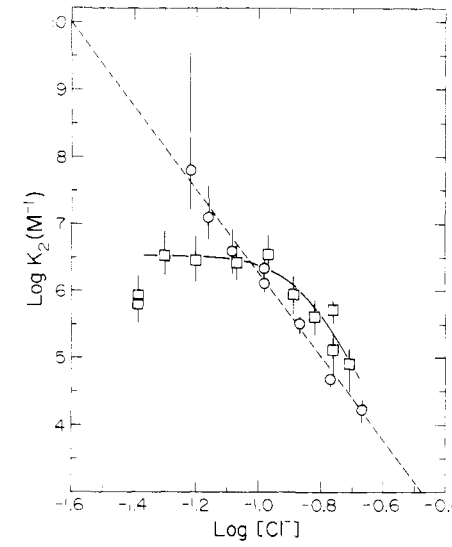

FIGURE 10: Dependence of the observed equilibrium constants for dimerization of holoenzyme on [Cl⁻]. The dashed line through the experimental points obtained in 0.01 M $MgCl_2$ (○) was obtained by linear least-squares regression. The solid curve through the data obtained in the absence of $MgCl_2$ (□) is the best fit for the completely cooperative model of anion binding to monomers.

equilibrium constants for holoenzyme aggregation in the presence and absence of Mg^{2+} have been calculated by assuming that the equilibrium is between a 13.7 ± 0.4 S monomer and a 22.0 ± 1.0 S dimer. (We stress that the validity of this assumption is uncertain due to our inability to reconcile the light-scattering data with the sedimentation data at high salt as well as our inability to positively identify the size of the aggregates formed at low salt.) Both sets of equilibrium constants are presented as a function of chloride in Figure 10.

The data in the presence of Mg^{2+} appear linear and are described by the least-squares equation

$$\log K_2\ (M^{-1}) = (0.7 \pm 0.6) - (5.6 \pm 0.9) \log [Cl^-] \quad (6)$$

for the range −1.22 < log [Cl⁻] < −0.71 (0.06 M < [Cl⁻] < 0.19 M). [Equilibrium constants could not be calculated from the values of $\bar{s}_{20,w}$ at the two lowest chloride concentrations (Figure 6) because dimerization is essentially complete, within experimental error, at the protein concentrations used.] The

slope of this line indicates that 2.8 ± 0.5 anions are released per holoenzyme monomer upon aggregation in this salt region.

As observed for the formation of core tetramers in the absence of Mg^{2+}, log K_2 for dimerization of holoenzyme in the absence of Mg^{2+} is not a linear function of log [Cl^-] over the entire range of chloride investigated. For direct comparison with the results for holoenzyme in the presence of Mg^{2+}, the equation for the best fit to the data in the linear region $-1.0 < \log [Cl^-] < 0.6$ ($0.1\ M < [Cl^-] < 0.25\ M$) is $\log K_2\ (M^{-1}) = (1.0 \pm 0.6) - (5.7 \pm 0.4) \log [Cl^-]$. The slope of the line in this region indicates that 2.8 ± 0.2 anions are released per holoenzyme monomer upon dimerization in the absence of Mg^{2+} for this limited range of salt concentration.

A more detailed analysis of the chloride dependence of log K_2 was attempted by using the two models described previously. The solid curve through the data is the weighted nonlinear least-squares fit to the completely cooperative model (eq 3). The equation of this curve is

$$\log K_2\ (M^{-1}) = (6.5 \pm 0.1) - 2 \log (1 + k_2[Cl^-]^{4.9 \pm 0.2}) \quad (7)$$

where $\log k_2 = 4.15 \pm 0.11$ for the range $-1.3 < \log [Cl^-] < -0.65$ ($0.05\ M < [Cl^-] < 0.22\ M$).

When the independent, identical sites model is used to fit the data, the qualitative features of the fit are similar to those described earlier for the core tetramer reaction. When all three parameters are allowed to vary, the sharp curvature of the data is reproduced only when n_1 is large ($>10^2$) and k_1 small ($<0.1\ M^{-1}$). If n_1 is constrained to a value consistent with physical binding (4.9, the value of n_2 providing the best fit to the completely cooperative model), the fit obtained (not shown) is described by the equation $\log K_2\ (M^{-1}) = (7.48 \pm 0.11) - 2(4.9) \log (1 + (3.50 \pm 0.27)[Cl^-])$. As for the core data, this fit is significantly less good than that of the completely cooperative model.

(*E*) *The Effect of Different Anions upon Core Aggregation Can Be Modeled as Resulting from Differences in the Intrinsic Anion Binding Constants.* Estimates of the affinity constants (k_2) for I^- and F^- for the completely cooperative model of anion binding may be obtained by fitting our data on the variation of K_4 with [I^-] or [F^-] in the absence of Mg^{2+} to eq 3 by using values of log K^0 and n_2 determined from the [Cl^-] data. We find that the equilibrium constants obtained as a function of [I^-] (not shown) yield $\log k_2\ (I^-) = 4.0 \pm 0.4$, and those obtained as a function of fluoride (also not shown) yield $\log k_2\ (F^-) = 2.5 \pm 0.5$ (both affinity constants are in units of $M^{-4.2}$). The theoretical curves through the data in Figure 5 have been generated by using an average total protein concentration of 0.29 mg/mL and using salt-dependent values of K_4 generated from eq 3 by using the parameters appropriate for each type of anion. The fit through the data seems adequate in view of the oversimplifications inherent in the all-or-none model. The order of these affinity constants [$k_2\ (I^-) > k_2\ (Cl^-) > k_2\ (F^-)$] is consistent with the ordering of the relative strength of interaction of these anions with proteins predicted by the Hofmeister series (von Hippel & Schleich, 1969). The ability to change the extent of aggregation at a given salt concentration by changing the anion has potential utility as an experimental tool to determine whether other properties of RNA polymerase such as DNA binding are affected by aggregation or by anions.

(*F*) *The Effect of* [Mg^{2+}] *on Core Aggregation Suggests a Net (Thermodynamic) Uptake of Two to Three Mg^{2+} per Octamer Formed.* To probe the effect of Mg^{2+} on the aggregation of core polymerase to octamers, we varied the concentration of $MgCl_2$ from 2 to 20 mM either in the absence of NaCl or at 0.05 M NaCl. In 2 mM $MgCl_2$ with no added NaCl, we obtained an $\bar{s}_{20,w}$ of 37.4 ± 0.4 S at a core concentration of 0.34 mg/mL. Since we estimate an $s^0_{20,w}$ of 30 ± 1 S for the core tetramer, this implies that 2 mM Mg^{2+} is sufficient to cause aggregation to proceed beyond the tetramer formed in the absence of Mg^{2+}. Using equilibrium constants calculated from sedimentation data in the absence of NaCl (duplicate points at 2, 5, 10, and 15 mM $MgCl_2$; data not shown), assuming a monomer–octamer stoichiometry, we found that d log K_8/d log [Mg^{2+}] is 2.5 ± 0.5, which implies that formation of an octamer from monomers is accompanied by a new uptake (in the thermodynamic sense) of two to three Mg^{2+} per octamer formed [see Record et al. (1978)]. It is unclear whether this increase represents ions involved in actual physical binding or is a net effect of the role of Mg^{2+} in increased electrostatic screening. The fact that the presence of Mg^{2+} does result in a change in the size of the largest aggregate formed suggests that some Mg^{2+} may site bind; however, the effect could be due only to increased Debye–Hückel screening of the aggregate. [Although the reaction involved is not completely analogous to those of interest here, Wishnia and co-workers (Wishnia & Boussert, 1977; Wishnia et al., 1975) have presented a useful discussion of the possible contribution of Mg^{2+} to electrostatic screening in ribosome formation.]

(*G*) *The Aggregation Reactions of both Core and Holoenzyme Are Only Weakly Dependent on pH.* The effect of pH on the dimerization of holoenzyme was examined at 0.20 M NaCl (data not shown). From pH 6.0 to pH 8.0, we measure a value for d log K_2/d pH of −0.2 ± 0.2 with or without Mg^{2+} in the buffers. The effect of pH on the aggregation equilibria of core polymerase was investigated at 0.20 M NaCl in both the presence and absence of Mg^{2+} for the same pH range. In the presence of Mg^{2+}, d log K_8/d pH is 0.6 ± 0.3; in the absence of Mg^{2+}, d log K_4/d pH is −1.0 ± 0.1. These small pH dependencies suggest that protonation of histidines or α-amino groups with p*K*s in this pH range is not a direct requirement for the aggregation reactions to proceed and that the variation in pH serves primarily to affect the overall net charge of RNA polymerase.

(*H*) *The Aggregation Equilibria of Core Polymerase Are Comparatively Insensitive to Temperature.* The effect of temperature on core octamer formation in the presence of 0.01 M Mg^{2+} at 0.08 M NaCl was examined. A 0.01 M Bicine buffer (pH 8.0 at 20 °C) was used in these experiments because the p*K* of Bicine has a smaller temperature coefficient than that of Tris (our standard buffer). At 20 °C, use of Bicine in place of Tris did not affect the results. The values of the $\bar{S}_{20,w}$ obtained at 6, 20, and 36 °C (data not shown) show a minimal temperature dependence. We calculate a van't Hoff enthalpy of −3 ± 1 kcal/mol of monomer incorporated into the octamer. [We observe only one boundary in the sedimentation data at these three temperatures. Hansen & McClure (1980) noted the presence of two sedimenting boundaries for core polymerase at 37 °C in 0.08 M KCl, 0.01 M $MgCl_2$, and 0.04 M Tris at pH 8.]

The temperature dependence of core tetramer formation was determined at 0.16 M NaCl (no Mg^{2+}) in 0.01 M Bicine (data not shown). Sedimentation coefficients were measured at four temperatures in the range 4–20 °C. The van't Hoff enthalpy is 1.3 ± 0.1 kcal/mol of monomer incorporated into the tetramer.

Discussion

Model for the Aggregation. A schematic diagram that summarizes our findings and is consistent with the limited structural data currently available is provided in Figure 11.

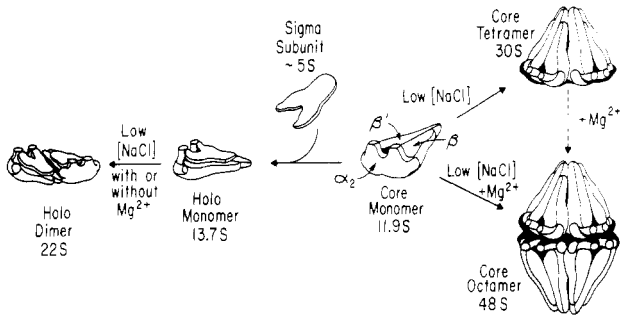

FIGURE 11: Schematic representation of the aggregation equilibria of core and holo RNA polymerase treated as monomer–j-mer reactions (see Results). Structures of core, σ, and holoenzyme monomer and dimer are based on small-angle X-ray scattering results (Meisenberger et al., 1980a–c, 1981; Heumann et al., 1982). Structures presented for the core tetramer and octamer are consistent with the sparse data currently available (see the text) but are otherwise entirely speculative.

(We wish to caution the reader that little is known about the three-dimensional structure of RNA polymerase or its aggregates and therefore, while Figure 11 is *consistent* with what is known, it is no more than a tentative model of the equilibria involved.) The core monomer has been presented as a trigonal unit, based on the structural model which has emerged from recent small-angle X-ray (Meisenberger et al., 1980a,c) and neutron scattering (Stöckel et al., 1980) studies performed at high salt in the absence of Mg^{2+}. Equally good fits to the scattering data were obtained when the elongated σ subunit (Meisenberger et al., 1980b) was attached to either the top or the bottom plane of the core monomer (Meisenberger et al., 1981). A side-by-side structure for the holoenzyme dimer was shown to be more consistent with the small-angle X-ray scattering data (in the absence of Mg^{2+}) than four other plausible structures (Heumann et al., 1982).

In the right-hand portion of Figure 11 we indicate two equally plausible explanations for the effect of Mg^{2+} on the size of the largest aggregate formed by core RNA polymerase. The Mg^{2+} may induce a conformational change in the core monomer, altering the types of interactions possible between monomers and thereby allowing aggregation to proceed via a pathway unavailable in the absence of Mg^{2+}. Alternatively the primary effect of the Mg^{2+} may be to allow two tetrameric units to interact with each other (path indicated by dotted arrow).

There is no information in the literature on the overall shape and structure of the octamer or the subunit interactions between the monomers composing it. The only information available concerning the structure of the tetramer is that β and/or β' are protected from protease digestion in the tetramer while α_2 is not (Lill & Hartmann, 1975). The arrangement of monomers within the tetramer that we have presented is one of the possibilities consistent with these data.

Anomalies in the Holoenzyme Results. We have considered a variety of explanations of the behavior of holoenzyme at high salt, where we see a single, nonreacting species in the ultracentrifuge but a heterogeneous scattering population in the QLS studies on the same samples. Sedimentation measurements were routinely performed after the light-scattering experiments to verify that exposure to the laser had not affected the protein. No evidence of a small fraction of fast-sedimenting material is observable in the sedimentation data. An excess of monomeric σ would contribute little to the scattering because of its small size. Free core has been shown to be a well-behaved monomer at these conditions, so its presence in solution would not contribute high molecular weight species. It seems unlikely that the inconsistency arises from the presence of dust in our scattering solutions. The high salt holo scattering samples were prepared in the same way as our high salt core samples, for which we encountered no difficulties. Another possible explanation is that holo aggregation, unlike core aggregation, could involve a significant molar volume change. If this were so, the aggregation producing the angular dependence of the QLS data at 1 atm might dissociate at the higher pressures generated by the centrifugal field. However, we have not detected a molar volume change large enough to account for this discrepancy. On the basis of values in the literature for the rotational correlation coefficient of holoenzyme (Wu et al., 1975) and the kinetic constants of the σ–core interaction (Wu et al., 1976), we have also rejected the possibility that rotational diffusion or fast σ exchange could be detected during the light-scattering experiment. At this time, we simply cannot reconcile the sedimentation and light-scattering data at high salt.

In addition to this paradox at high salt, there are unanswered questions concerning holoenzyme at low salt. We were unable to confirm the low salt molecular weight reported by Pilz et al. (1972) for the species in the presence of Mg^{2+}. If the 13.7 S species is the holoenzyme monomer, one would predict (assuming that $S \propto M^{2/3}$) that its dimer would have an $s^0_{20,w}$ of ~22 S. This value is consistent with the $\bar{s}_{20,w}$ values we have measured at the lowest chloride concentrations used to within the estimated uncertainties. In the absence of Mg^{2+}, the plateau region (at ~18.8 S) observed below 0.11 M Cl^- may indicate the presence of a dimer of an alternate conformation to that found in the presence of Mg^{2+}. There are some indications that Mg^{2+} may influence the conformation assumed by holoenzyme (Fisher & Blumenthal, 1980). Alternatively, the same dimerization process may be occurring with or without Mg^{2+}, but in the absence of Mg^{2+}, the increase in $\bar{s}_{20,w}$ expected for elevated levels of aggregation at lower salts may be counterbalanced by either the primary charge effect or a decrease in the σ–core equilibrium constant. Observation of a complex containing two cores and only one σ has been claimed at low salt in the absence of Mg^{2+} (Savotchkina & Beabealashvilly, 1979). We have performed an experiment using a Bio-Gel A1.5m column to determine whether σ is lost at 0.05 M NaCl in the absence of Mg^{2+}. The aggregate which emerged from the column was identical in σ content to the holoenzyme loaded onto it (R. R. Burgess, unpublished data). This experiment does not conclusively eliminate the possible existence of the two core–one σ complex. It may only indicate that the free σ exchanges sufficiently rapidly with the bound σ to allow it to run through the column with the complex.

It is possible that the very low $\bar{s}_{20,w}$ found at 0.04 M Cl^- without Mg^{2+} was artificially depressed below its actual value by the primary charge effect whereas data obtained at higher Cl^- or in the presence of Mg^{2+} were not. The primary charge effect is a sedimentation artifact arising from the differential sedimentation of a charged macromolecule and its counterions in solutions of insufficient ionic strength to minimize the potential gradient which forms. The effect results in depression of the $\bar{s}_{20,w}$ observed for the species (Schachman, 1959). On the basis of the amino acid content and/or sequence of the subunits (Burgess, 1976; Ovchinnikov et al., 1977, 1981; Burton et al., 1981), both forms of the enzyme would be predicted to have a substantial net negative charge at pH 8.0 (approximately −100 for holoenzyme and −70 for core polymerase). The primary charge effect is poorly understood at a quantitative level. Typically, however, buffers of ionic strength greater than 0.05–0.1 M are considered sufficient to

eliminate this artifact. If this observation is applicable to RNA polymerase, then only the data collected at the very lowest chloride concentrations (<0.05 M) would be affected.

Interpretation of the Effect of Anions on the Aggregation Equilibria. The observed effect of electrolyte on the aggregation equilibria investigated here could arise from the differential interactions of electrolyte ions and/or solvent with the monomers and aggregates. The possible origins of an electrolyte effect have been considered in detail elsewhere (Record et al., 1978). The following contributions have been identified: (i) differential cation and/or anion binding, (ii) differential Debye–Hückel screening effects on the protein by the electrolyte ions, and (iii) salt effects on differential hydration. We assume that the effect of differential hydration in this investigation is negligible since the transitions from monomer to aggregate occur at relatively low electrolyte concentrations (Tanford, 1969; Record et al., 1978). Inasmuch as we observe a specific effect upon interchanging the anion, but no effect upon interchanging the cation (Figure 5), it is reasonable to conclude that the observed effect arises from a specific anion interaction. Since both core and holo RNA polymerase possess a net negative charge (Burton et al., 1981), the observed effect is most probably due to physical binding of the anions rather than to differential screening.

We have considered two different models to describe the dependence of the aggregation reactions of RNA polymerase on $[Cl^-]$ in the absence of Mg^{2+}. A first model in which n_1 independent, identical anion binding sites available on the j monomers are occluded upon aggregation to the j-mer was found to fit the data poorly when n_1 was constrained to have a value consistent with true anion binding rather than with preferential solvation.

A second model in which a class of n_2 sites for the cooperative binding of anions to each monomer are lost upon aggregation was found to provide an excellent fit to both sets of data in the absence of Mg^{2+}. Such cooperativity can arise in two ways, it can be either lattice or ligand based. Because the ligands are simple anions, ligand–ligand interactions would be expected to be intrinsically anticooperative as a result of repulsive electrostatic interactions between the anions. The simplest lattice-based mechanism which could produce the apparent cooperative effect of anions on the aggregation reaction is an equilibrium between two possible monomer conformations, in which one conformation (P*) binds anions to a class of n_3 independent, identical sites but does not aggregate, while the other conformation (P) aggregates readily but does not bind anions. In this third model, anions act as allosteric effectors of the monomer conformational equilibrium. [Anion effects on the ligand binding, aggregation, and allosterism of hemoglobin have been documented (Benesch et al., 1969; Haire & Hedlund, 1977; Record et al., 1978; Chu & Ackers, 1981). A quantitative molecular analysis of these anions effects has not been attempted.]

This model is described by the following two reactions:

$$P^* \underset{}{\overset{K_C}{\rightleftharpoons}} P \qquad K_C = K_C^0(1 + k_3[X^-])^{-n_3}$$

$$jP \overset{K_{agg}}{\rightleftharpoons} A \qquad K_{agg} = K_{agg}^0$$

The observed equilibrium constant, K_{obsd}, is

$$K_{obsd} = \frac{[A]}{[P + P^*]^j} = K_{agg}^0[1 + (K_C^0)^{-1}(1 + k_3[X^-])^{n_3}]^{-j} \tag{8}$$

where $[P + P^*]$ is the total concentration of free monomer. When $k_3[X^-] > 1$, this expression reduces to

$$\log K_{obsd} = \log K_{agg}^0 - j \log \left(1 + \frac{k_3^{n_3}}{K_C^0}[x^-]^{n_3} \right) \tag{9}$$

Comparison of eq 9 with eq 3 demonstrates that in the limit $k_3[X^-] > 1$ the allosteric model reduces to the completely cooperative model with $k_2 = k_3^{n_3}/K_C^0$ and $n_2 = n_3$.

For the data of both core and holoenzyme, when the number of anion binding sites is constrained to equal the number of sites in the respective completely cooperative fits, we find that the affinity constant for the allosteric sites (k_3) is sufficiently large in each case to reduce the allosteric model to the completely cooperative model.[3] For core polymerase, the parameter values obtained when the constraint $n_3 = 4.2$ was imposed are $\log K_{agg}^0\ (M^{-3}) = 20.6 \pm 0.1$, $k_3 = (1.0 \pm 0.1) \times 10^3\ M^{-1}$, and $K_C^0 = (9.4 \pm 0.6) \times 10^8$. When n_3 is constrained at 4.9 for holoenzyme, we obtain the following best-fit parameter values: $\log K_{agg}^0\ (M^{-1}) = 6.5 \pm 0.2$, $K_C^0 = 10^{17}$, and $k_3 = 2 \times 10^4\ M^{-1}$.

The values of $\log K_{obsd}$ for the aggregation of both core and holoenzyme in the presence of Mg^{2+} appear linear in $\log [Cl^-]$. Consequently, we are unable to infer anything about the molecular details of these two aggregation equilibria. In particular, we are unable to determine whether an allosteric effect comparable to that which we have invoked in the absence of Mg^{2+} occurs in the presence of Mg^{2+}.

Application to the Binding of RNA Polymerase to DNA in Vitro. Two aspects of our work may have implications for in vitro investigations of the interaction of RNA polymerase and DNA. These are (1) our quantification of the effects of protein concentration and ion concentrations on the extent of aggregation of the enzyme and (2) our conclusion that an anion-linked conformational equilibrium may occur in the protomeric forms of core and holoenzyme in the range of ion concentrations commonly used in vitro.

One of our goals has been to provide an experimentally useful quantitative guide to the extent of aggregation of RNA polymerase as a function of enzyme concentration and ionic conditions. Such an empirical guide is provided in eq 4–5 for core and in eq 6–7 for holoenzyme, in combination with our data on the Mg^{2+} and pH dependences of these equilibria. These experiments have been performed at 3% (v/v) glycerol; the effect of glycerol content on the aggregation equilibria has not been investigated.

The various techniques that have been applied to the study of the specific and/or nonspecific DNA-binding properties of RNA polymerase require quite different amounts of enzyme. Particularly at low salt concentrations, these different techniques may be examining the properties of very different enzyme populations. To illustrate this, we compare the extent of dimerization of holoenzyme (at 0.05 M NaCl and 0.01 M $MgCl_2$) predicted by eq 7 at the typical protein concentration used in four different techniques: transcription (e.g., Maquat & Reznikoff, 1978), 5×10^{-12} M holoenzyme, 0.01% dimer; filter binding (e.g., Hinkle & Chamberlin, 1972; Strauss et

[3] One potential problem in analyzing our data with the model in which two conformations exist for the monomers of core and holoenzyme is that these two conformations might be expected to have different values of $s^0_{20,w}$. This would have no impact on our analysis if the difference in these two values were within the limits of our experimental uncertainty in determining the $s^0_{20,w}$ of the monomer. Kirschner & Schachman (1971) found changes of 0.5–3% in the $s^0_{20,w}$ of aspartate transcarbamylase upon ligand-induced conformational changes. For both core and holoenzyme, this percentage of variation would be within the limits of our uncertainty for the monomer $s^0_{20,w}$.

al., 1980), 10^{-9} M holoenzyme, 1.5% dimer; abortive initiation (McClure, 1980), 5×10^{-8} M holoenzyme, 33% dimer; UV absorbance at 280 nm, 10^{-6} M holoenzyme, 77% dimer. Increasing the [NaCl] to 0.15 M reduces the extent of dimerization for this range of protein concentrations to 0–10% dimer. Obviously, if the monomers and aggregates have different DNA-binding properties, these four techniques studying "identical systems" might yield widely differing values of the binding constant at a fixed set of solution conditions. Additionally, if the position of the aggregation equilibrium is perturbed by binding to DNA, then the measured value of d log K_{obsd}/d log [NaCl] for the DNA-binding reaction would include a contribution from the differential interaction of the monomers and aggregate with Cl^-. These four techniques might therefore observe widely varying values for d log K_{obsd}/d log [NaCl].

Most of the in vitro studies of the nonspecific binding of RNA polymerase to double-stranded DNA have used sufficiently low concentrations of core polymerase or holoenzyme to be free of significant amounts of aggregation at the ionic conditions employed (Revzin & Woychik, 1981; Lohman et al., 1980; Kadesch et al., 1980; deHaseth et al., 1978). On the other hand, all of these studies were performed at NaCl concentrations in the range where we infer the existence of a transition in the monomer conformation. Using the parameters for the conformational transitions of core and holoenzyme obtained with the allosteric model, we calculate for both forms of the enzyme that at least 90% of the protomer population would be in the "low salt" conformation below 0.08 M Cl^- and that at least 90% of the population would be in the "high salt" form above 0.3 M Cl^-, in the absence of Mg^{2+}. [The aggregation transitions (Figures 1, 5, and 6) serve as an indicator of the extent of conversion of these forms of the protomer as a function of anion concentration.] It is possible that the two monomer conformations may possess different DNA-binding properties. The involvement of up to four anions in the monomer conformational change of core and up to five in that of holoenzyme implies that if such a conformational change is involved in the binding of RNA polymerase to DNA, anion effects on the protein could provide a significant contribution to the total observed salt dependence of the DNA-binding reaction. An investigation of the effects of anions on the DNA binding of RNA polymerase is in progress in this laboratory (S. L. Shaner and K. S. Lee, umpublished results); dramatic anion effects on the magnitude of the binding constant have been observed for the binding of *lac* repressor to operator DNA (Barkley et al., 1981) and of gene 32 protein to homopolynucleotides (Kowalczykowski et al., 1981).

Acknowledgments

We thank Paul Melançon for many helpful discussions and criticism of an earlier draft of the manuscript, Laura Unger for her assistance with Figure 11, and Drs. M. J. Chamberlin and A. A. Travers for their comments on the manuscript.

References

Amis, E. J. (1981) Ph.D. Thesis, University of Wisconsin, Madison, WI.

Barkley, M. D., Lewis, P. A., & Sullivan, G. E. (1981) *Biochemistry 20*, 3842–3851.

Beabealashvilly, R. Sh., & Savotchkina, L. P. (1973) *Biochim. Biophys. Acta 294*, 434–441.

Benesch, R. E., Benesch, R., & Yu, C. I. (1969) *Biochemistry 8*, 2567–2571.

Berg, D., & Chamberlin, M. (1970) *Biochemistry 9*, 5055–5064.

Berne, B. J., & Pecora, R. (1976) *Dynamic Light Scattering*, Wiley-Interscience, New York.

Bloomfield, V. A., & Lim, T. K. (1978) *Methods Enzymol. 48*, 415–494.

Brehm, G. A., & Bloomfield, V. A. (1975) *Macromolecules 8*, 663–665.

Burgess, R. R. (1969) *J. Biol. Chem. 244*, 6160–6167.

Burgess, R. R. (1971) *Annu. Rev. Biochem. 140*, 711–740.

Burgess, R. R. (1976) in *RNA Polymerase* (Losick, R., & Chamberlin, M. J., Eds.) pp 69–100, Cold Spring Harbor Laboratory, Cold Spring Harbor, NY.

Burgess, R. R., & Jendrisak, J. J. (1975) *Biochemistry 14*, 4634–4638.

Burgess, R. R., Travers, A. A., Dunn, J. J., & Bautz, E. K. F. (1969) *Nature (London) 221*, 43–46.

Burton, Z., Burgess, R. R., Lin, J., Moore, D., Holder, S., & Gross, C. A. (1981) *Nucleic Acids Res. 9*, 2889–2903.

Chamberlin, M. J. (1976) in *RNA Polymerase* (Losick, R., & Chamberlin, M. J., Eds.) pp 159–191, Cold Spring Harbor Laboratory, Cold Spring Harbor, NY.

Chamberlin, M. J., Nierman, W. C., Wiggs, J., & Neff, N. (1979) *J. Biol. Chem. 254*, 10061–10069.

Chu, A. H., & Ackers, G. K. (1981) *J. Biol. Chem. 256*, 1199–1205.

deHaseth, P. L., Lohman, T. M., Burgess, R. R., & Record, M. T., Jr. (1978) *Biochemistry 17*, 1612–1622.

Eisenberg, H. (1976) *Biological Macromolecules and Polyelectrolytes in Solution*, Oxford University Press, London.

Fisher, R., & Blumenthal, T. (1980) *J. Biol. Chem. 255*, 11056–11062.

Fujita, H. (1975) *Foundations of Ultracentrifugal Analysis*, Wiley, New York.

Gekko, K., & Timasheff, S. N. (1981a) *Biochemistry 20*, 4667–4676.

Gekko, K., & Timasheff, S. N. (1981b) *Biochemistry 20*, 4677–4686.

Goldberg, R. J. (1953) *J. Phys. Chem. 57*, 194–202.

Haire, R. N., & Hedlund, B. E. (1977) *Proc. Natl. Acad. Sci. U.S.A. 74*, 4135–4138.

Hansen, U. M., & McClure, W. R. (1980) *J. Biol. Chem. 225*, 9556–9563.

Harrington, W. F., & Kegeles, G. (1973) *Methods Enzymol. 27*, 306–345.

Hess, V. L., & Szabo, A. (1979) *J. Chem. Educ. 56*, 289–293.

Heumann, H., Meisenberger, O., & Pilz, I. (1982) *FEBS Lett. 138*, 273–276.

Hinkle, D. C., & Chamberlin, M. J. (1972) *J. Mol. Biol. 70*, 157–185.

Holloway, R. R., & Cox, D. J. (1974) *Arch. Biochem. Biophys. 160*, 595–602.

Josephs, R., & Harrington, W. F. (1968) *Biochemistry 7*, 2834–2897.

Kadesch, T. R., Williams, R. C., & Chamberlin, M. J. (1980) *J. Mol. Biol. 136*, 65–78.

Kegeles, G., Rhodes, L., & Bethune, J. L. (1967) *Proc. Natl. Acad. Sci. U.S.A. 58*, 45–51.

Kirschner, M. W., & Schachman, H. K. (1971) *Biochemistry 10*, 1919–1926.

Klotz, I. M., Darnell, D. W., & Langerman, N. R. (1975) *Proteins (3rd Ed.) 1*, 194–411.

Koppel, D. E. (1972) *J. Chem. Phys. 57*, 4814–4820.
Kowalczykowski, S. C., Lonberg, N., Newport, J. W., & von Hippel, P. H. (1981) *J. Mol. Biol. 145*, 75–104.
Lill, H. R., & Hartmann, G. R. (1975) *Eur. J. Biochem. 54*, 45–53.
Lohman, T. M., Wensley, C. G., Cina, J., Burgess, R. R., & Record, M. T., Jr. (1980) *Biochemistry 19*, 3516–3522.
Lowe, P. A., Hager, D. A., & Burgess, R. R. (1979) *Biochemistry 18*, 1344–1352.
Maquat, L. E., & Reznikoff, W. S. (1978) *J. Mol. Biol. 125*, 467–490.
McClure, W. R. (1980) *Proc. Natl. Acad. Sci. U.S.A. 77*, 5634–5638.
Meisenberger, O., Heumann, H., & Pilz, I. (1980a) *FEBS Lett. 122*, 117–120.
Meisenberger, O., Pilz, I., & Heumann, H. (1980b) *FEBS Lett. 112*, 39–41.
Meisenberger, O., Pilz, I., & Heumann, H. (1980c) *FEBS Lett. 120*, 57–60.
Meisenberger, O., Heumann, H., & Pilz, I. (1981) *FEBS Lett. 123*, 22–24.
Ovchinnikov, Yu. A., Lipkin, V. A., Modyanov, N. N., Chertov, O., & Smirnov, Yu, V. (1977) *FEBS Lett. 76*, 108–111.
Ovchinnikov, Yu. A., Monastryrskaya, G. S., Gubanov, V. V., Guryev, S. O., Chertov, O., Modyanov, N. N., Grinkevich, V. A., Markarova, I. A., Marchenko, T. V., Polovnikova, I. N., Lipkins, V. M., & Sverdlow, E. D. (1981) *Eur. J. Biochem. 116*, 621–629.
Pilz, I., Kratky, O., & Rabussay, D. (1972) *Eur. J. Biochem. 28*, 205–220.
Record, M. T., Jr., Anderson, C. F., & Lohman, T. M. (1978) *Q. Rev. Biophys. 11*, 103–178.
Revzin, A., & Woychik, R. P. (1981) *Biochemistry 20*, 250–256.
Richardson, J. P. (1966) *Proc. Natl. Acad. Sci. U.S.A. 55*, 1616–1623.
Savotchkina, L. P., & Beabealashvilly, R. Sh. (1979) *Mol. Biol. (Engl. Transl.) 13*, 509–518.
Schachman, H. K. (1959) *Ultracentrifugation in Biochemistry*, Academic Press, New York.
Schellman, J. A. (1975) *Biopolymers 14*, 999–1018.
Schellman, J. A. (1978) *Biopolymers 17*, 1305–1322.
Stevens, A., Emery, A. J., Jr., & Sternberger, N. (1966) *Biochem. Biophys. Res. Commun. 24*, 929–936.
Stöckel, P., May, R., Strell, I., Cejka, Z., Hoppe, W., Heumann, H., Zillig, W., & Crespi, H. (1980) *Eur. J. Biochem. 112*, 411–417.
Strauss, H. S., Burgess, R. R., & Record, M. T., Jr. (1980) *Biochemistry 19*, 3504–3515.
Tanford, C. (1969) *J. Mol. Biol. 39*, 539–544.
Teller, D. C. (1973) *Methods Enzymol. 27*, 346–441.
TenEyck, L. F., & Kauzmann, W. (1967) *Proc. Natl. Acad. Sci. U.S.A. 58*, 888–894.
Travers, A. A., Lamond, A. J., & Mace, H. A. F. (1982) in *Promoters: Structure and Function* (in press).
van Holde, K. (1975) *Proteins (3rd Ed.) 1*, 225–291.
von Hippel, P. H., & Schleich, T. (1969) *Acc. Chem. Res. 2*, 257–265.
Wensley, C. G. (1977) Ph.D. Thesis, University of Wisconsin, Madison, WI.
Wishnia, A., & Boussert, A. S. (1977) *J. Mol. Biol. 116*, 577–591.
Wishnia, A., Boussert, A., Graffe, M., Dessen, Ph., & Grunberg-Manago, M. (1975) *J. Mol. Biol. 93*, 499–515.
Wu, C.-W., Yarbrough, L. R., Hillel, Z., & Wu, F. Y.-H. (1975) *Proc. Natl. Acad. Sci. U.S.A. 72*, 3019–3023.
Wu, F. Y.-H., Yarbrough, L. R., & Wu, C.-W. (1976) *Biochemistry 15*, 3254–3258.
Wyman, J. (1964) *Adv. Protein Chem. 19*, 223–286.